SLAC-PUB-7196
June 1996

Preliminary Measurement of the Charged Multiplicities in b, c and Light Quark Events from Z^0 Decays*

The SLD Collaboration**
Stanford Linear Accelerator Center
Stanford University, Stanford, CA 94309

* This work was supported by Department of Energy contracts: DE-FG02-91ER40676 (BU), DE-FG03-91ER40618 (UCSB), DE-FG03-92ER40689 (UCSC), DE-FG03-93ER40788 (CSU), DE-FG02-91ER40672 (Colorado), DE-FG02-91ER40677 (Illinois), DE-AC03-76SF00098 (LBL), DE-FG02-92ER40715 (Massachusetts), DE-AC02-76ER03069 (MIT), DEFG06-85ER40224 (Oregon), DEAC03-76SF00515 (SLAC), DE-FG05-91ER40627 (Tennessee), DE-FG02-95ER40896 (Wisconsin), DE-FG02-92ER40704 (Yale); National Science Foundation grants: PHY-91-13428 (UCSC), PHY-89-21320 (Columbia), PHY-92-04239 (Cincinnati), PHY-88-17930 (Rutgers), PHY-88-19316 (Vanderbilt), PHY-92-03212 (Washington); the UK Science and Engineering Research Council (Brunel and RAL); the Istituto Nazionale di Fisica Nucleare of Italy (Bologna, Ferrara, Frascati, Pisa, Padova, Perugia); and the Japan-US Cooperative Research Project on High Energy Physics (Nagoya, Tohoku).

Ref PA04-042
Submitted to the 28th International Conference on High Energy Physics, Warsaw, Poland, July 25-31,1996

ABSTRACT

Average charged multiplicities have been measured separately in *b, c* and light quark *(u, d, s)* events from Z^0 decays measured in the SLD experiment. Impact parameters of charged tracks were used to select enriched samples of *b* and light quark events, and reconstructed charmed mesons were used to select *c* quark events. We measured the charged multiplicities: $\overline{n}_{uds}$ = 20.21 ± 0.10 (stat.) ± 0.17 (syst.), $\overline{n}_c$ = 21.28 ± 0.46 $(\text{stat.})^{+0.38}_{-0.33}$ (syst.) and $\overline{n}_b$ = 23.14 ± 0.10 $(\text{stat.})^{+0.35}_{-0.34}$ (syst.), from which we derived the differences between the total average charged multiplicities of *c* or *b* quark events and light quark events: $\Delta\overline{n}_c$ = 1.07 ± 0.47 $(\text{stat.})^{+0.36}_{-0.30}$ (syst.) and $\Delta\overline{n}_b$ = 2.93 ± 0.14 $(\text{stat.})^{+0.30}_{-0.29}$ (syst.). We compared these measurements with those at lower center-of-mass energies and with perturbative QCD predictions. These combined results are in agreement with the QCD expectations and disfavor the hypothesis of flavor-independent fragmentation.

1 Introduction

Heavy quark *(Q=c,b)* systems provide important laboratories for experimental tests of the theory of strong interactions, quantum chromodynamics (QCD). Since the large quark mass M_Q acts as a cutoff for soft gluon radiation, some properties of these systems can be calculated accurately in perturbative QCD. In other cases, however, where QCD calculations assume massless quarks, the products of heavy hadron decays can complicate the comparison of data with the predictions for massless partons. It is therefore desirable to measure properties of both light- and heavy-quark systems as accurately as possible.

Here we consider one of the most basic observable properties of high energy particle interactions, the multiplicity of charged hadrons produced in the final state. We consider hadronic Z^0 decays, which are believed to proceed via creation of a primary quark-antiquark pair, $Z^0 \to q\bar{q}$, which subsequently undergoes a fragmentation process to produce the observed jets of hadrons. If the primary event flavor *q* can be identified experimentally, one can measure the average charged multiplicity $\overline{n}_q$ in events of that flavor, for example *q = b, c, uds,* where *uds* denotes the average over events of the types $Z^0 \to u\bar{u}, d\bar{d}$, and $s\bar{s}$. These are not only important properties of Z^0 decays, but, if the average decay multiplicity of the *leading* hadrons that contain the primary heavy quark or antiquark is subtracted from $\overline{n}_Q$ to yield the average *non-leading* multiplicity, can also be used to test our understanding of the quark fragmentation process and its dependence on the quark mass. The hypothesis of flavor-independent fragmentation [1, 2] implies that this non-leading multiplicity in $e^+e^- \to Q\bar{Q}$ ("heavy quark") events at center-of-mass (c.m.) energy *W* should be equal to the total multiplicity in $e^+e^- \to u\bar{u}, d\bar{d}$, and $s\bar{s}$ ("light quark") events at a lower c.m. energy given by the average energy of the non-leading system, $E_{nl} = (1 - \langle x_{E_Q} \rangle)W$, where $\langle x_{E_Q} \rangle = 2E_Q/W$ is the mean fraction of the beam energy carried by a heavy hadron of flavor *Q*.

Perturbative QCD predictions have been made [3] of the multiplicity difference between heavy- and light-quark events, $\Delta\overline{n}_Q = \overline{n}_Q - \overline{n}_{uds}$. In this case the suppression

of soft gluon radiation caused by the heavy quark mass leads to a depletion of the non-leading multiplicity, and results in the striking prediction that $\Delta\overline{n}_Q$ is independent of W at the level of ±0.1 tracks. Numerical predictions of $\Delta\overline{n}_b = 5.5 \pm 1.3$ and $\Delta\overline{n}_c = 1.7 \pm 1.1$ were also given [3]. More recently, improved calculations have been performed [4], confirming that the energy-dependence is expected to be very small and predicting $\Delta\overline{n}_b = 3.53 \pm 0.23$ and $\Delta\overline{n}_c = 1.02 \pm 0.24$ at $W = M_{Z^0}$.

In our previous paper [5] we measured $\overline{n}_b$ and $\Delta\overline{n}_b$ using the sample of about 10,000 hadronic Z^0 decays recorded by the SLD experiment in the 1992 run. By comparing with similar measurements at lower c.m. energies [1, 6, 7, 8] we found that $\Delta\overline{n}_b$ was consistent with an energy-independent value, and in agreement with the prediction of [3]. This result was subsequently confirmed by the DELPHI [9] and OPAL [10] Collaborations. The dominant uncertainty in our measurement resulted from lack of knowledge of the charged multiplicity in $Z^0 \to c\bar{c}$ events, $\overline{n}_c$. Here we present simultaneous measurements of $\overline{n}_b, \overline{n}_c$ and $\overline{n}_{uds}$ based upon the sample of about 160,000 hadronic Z^0 decays collected by SLD between 1992 and 1995, and using the SLD micro-vertex detector and tracking system for flavor separation. By measuring $\overline{n}_c$ and $\overline{n}_{uds}$ directly we have reduced the systematic uncertainty on $\Delta\overline{n}_b$ substantially, and have also derived $\Delta\overline{n}_c$, which allows us to compare with the QCD predictions for the charm system and with the only other measurement of this quantity [10] at the Z^0. This measurement supersedes our previous measurements of $\overline{n}_b$ and $\Delta\overline{n}_b$ [5].

2 Apparatus and Hadronic Event Selection

The e^+e^- annihilation events produced at the Z^0 resonance by the SLAC Linear Collider (SLC) were recorded using the SLC Large Detector (SLD). A general description of the SLD can be found elsewhere [1 1]. The trigger and selection criteria for isolating hadronic Z^0 boson decays are described elsewhere [12].

The analysis presented here used the charged tracks measured in the central drift

chamber (CDC) [13] and in the vertex detector (VXD) [14]. A set of cuts was applied to the data to select well-measured tracks, which were used for multiplicity counting, and events well-contained within the detector acceptance. The well-measured tracks were required to have (i) a closest approach transverse to the beam axis within 5 cm, and within 10 cm along the axis from the measured interaction point; (ii) a polar angle θ with respect to the beam axis within $|\cos\theta| < 0.80$; and (iii) a momentum transverse to the beam axis $p_\perp > 0.15$ GeV/c. Events were required to have (i) a minimum of seven such tracks; (ii) a thrust axis [15] direction within $|\cos\theta_T| < 0.71$; and (iii) a total visible energy E_{vis} of at least 20 GeV, which was calculated from the selected tracks assigned the charged pion mass; 114,499 events passed these cuts. The background in the selected event sample was estimated to be $0.1 \pm 0.1\%$, dominated by $Z^0 \to \tau^+\tau^-$ events.

While the multiplicity measurement relied primarily on information from the CDC, the additional information from the VXD provided the more accurate impact parameter measurement, and *D* meson vertex reconstruction, used for selecting samples enriched in light *(u, d, s)* and *b* events, and *c* events, respectively. In addition to the requirements for well-measured tracks, "impact parameter quality" tracks were required to have (i) at least one VXD hit; (ii) a closest approach transverse to the beam axis within 0.3 cm, and within 1.5 cm along the axis from the measured interaction point; (iii) at least 40 CDC hits, with the first hit at a radius less than 39 cm; (iv) an error on the impact parameter transverse to the beam axis less than 250 μm; (v) a fit quality of the CDC track $\chi^2/d.o.f$ < 5; and (vi) a fit quality of the combined CDC+VXD track $\chi^2/d.o.f$ < 5. We also removed tracks from candidate K^0_s and Λ decays and γ-conversions found by kinematic reconstruction of two-track vertices.

All impact parameters used in this analysis were for tracks projected into the *(x – y)* plane perpendicular to the beam axis, and were measured with respect to an average primary vertex. The average primary vertex was derived from fits to $\sim$30 sequential hadronic events close in time to the event under study, with a measured precision of

$\sigma_{PV} = (7 \pm 2)\mu$m [16]. The impact parameter δ was derived by applying a sign to the distance of closest approach such that δ is positive when the vector from the primary vertex to the point at which the track intersects the thrust axis makes an acute angle with respect to the track direction. Including the uncertainty on the average primary vertex the measured impact parameter uncertainty σ_δ for the overall tracking system approaches 11 μm for high momentum tracks, and is 76 μm at $p_\perp\sqrt{\sin\theta}$=1 GeV/c [16].

3 Selection of Flavor-Tagged Samples

We divided each event into two hemispheres separated by the plane perpendicular to the thrust axis. We then applied three flavor tags to each hemisphere. In order to reduce potential tagging bias we measured the average charged multiplicity in hemispheres opposite to those tagged. Impact parameters of charged tracks were used to select enriched samples of *b* or light quark hemispheres, and reconstructed charmed mesons were used to select *c* quark hemispheres.

In each hemisphere we counted the number of impact parameter quality tracks n_{sig} that had an impact parameter significance of $\delta_{norm} = \delta/\sigma_\delta$ >3.0. Fig. 1 shows the distribution of n_{sig} upon which is superimposed a Monte Carlo simulated distribution in which the flavor composition is shown. For our Monte Carlo study we used the JETSET 7.4 event generator [17] with parameter values tuned to hadronic e^+e^- annihilation data [18], combined with a simulation of *B*- decays tuned to $\Upsilon(4s)$ data [16], and a simulation of the SLD. A more detailed discussion of flavor tagging using impact parameters can be found in [16]. The Monte Carlo simulation reproduces the data well and shows that most light quark hemispheres have n_{sig}=0 and that the $n_{sig}\geq$3 region is dominated by *b* quark hemispheres. Hemispheres were tagged as light or *b* quark by requiring $n_{sig} = 0$ or $n_{sig} \geq 3$, respectively. Table 1 shows the number of light and *b* quark tagged hemispheres and their flavor compositions estimated from the simulation.

From Fig. 1 it is clear that an impact parameter tag does not provide a high-

		uds-tag	*c*-tag	*b*-tag
# hem.		154,151	976	9,480
composition	*uds*	0.752±0.001 ±0.004	0.074±0.002 ±0.014	0.014±0.001 ±0.001
	c	0.158±0.001 ±0.006	0.640±0.008 ±0.025	0.048±0.001 ±0.005
	b	0.089±0.001 ±0.004	0.286±0.005 ±0.022	0.938±0.001 ±0.006

Table 1. Numbers of hemispheres and fractional compositions of *uds*, *c* and *b* quarks in the tagged hemispheres. The first quoted errors represent the errors due to the limited size of the Monte Carlo sample and the second are due to the uncertainties from the modelling of heavy hadron production and decay.

purity sample of *c* quark hemispheres. For this purpose we required at least one prompt D^{*+} or D^+ meson[1] reconstructed in a hemisphere. This tag is similar to that described in [19]. The D^{*+} mesons were identified using the decay $D^{*+} \to \pi_s^+ D^0$, where π_s^+ is a low-momentum pion and the D^0 decays via $D^0 \to K^-\pi^+$ ("three-prong"), $D^0 \to K^-\pi^+\pi^0$ ("satellite"), or $D^0 \to K^-\pi^+\pi^+\pi^-$ ("five-prong") modes. The D^+ mesons were identified using the decay mode $D^+ \to K^-\pi^+\pi^+$. D meson candidates were formed from all combinations of well-measured tracks with at least one VXD hit. D^0 candidates were formed by combining two (for the three-prong and satellite modes) or four (for the five-prong mode) charged tracks with zero net charge, and by assigning the K^- mass to one of the particles and π^+ mass to the others.

For D^{*+} candidates, we first required a candidate D^0 in the mass range 1.765 $\mathrm{GeV/c^2} < M_{D^0}^{cand.} < 1.965$ $\mathrm{GeV/c^2}$ (three-prong), 1.815 $\mathrm{GeV/c^2} < M_{D^0}^{cand.} < 1.915$ $\mathrm{GeV/c^2}$ (five-prong), or 1.500 $\mathrm{GeV/c^2} < M_{D^0}^{cand.} < 1.700$ $\mathrm{GeV/c^2}$ (satellite). D^{*+} candidates were then required to pass either a set of kinematic cuts or a set of decay length cuts to suppress combinatorial backgrounds and backgrounds from $B \to D^{*+}$ decays. The kinematic cuts are: (i) $|\cos\theta_{KD^0}| < 0.9$ (three-prong and satellite modes) and $|\cos\theta_{KD^0}| < 0.8$ (five-prong mode), where θ_{KD^0} is the angle between the D^0 direction in the laboratory frame and the *K* direction in the D^0 rest frame, (ii) $p_{\pi_s^+} > 1$ GeV/c,

[1] Charge-conjugate cases are always implied.

and (iii) $x_{E_{D^{*+}}}$ >0.4 for the three-prong and satellite modes and $x_{E_{D^{*+}}}$ >0.5 for the five-prong mode, where $x_{E_{D^{*+}}} = 2E_{D^{*+}}/W$ and $E_{D^{*+}}$ is the D^{*+} energy. For the decay length analysis we performed a fit of the D^0 tracks to a common vertex and calculated the decay length, L^0, between the primary vertex and this D^0 decay vertex, and its error, σ_{L^0}. The decay length cuts are: (i) a χ^2 probability > 1% for the vertex fit to the D^0 tracks, (ii) a decay length significance L^0/σ_{L^0} >2.5, (iii) the two-dimensional impact parameter of the D^0 momentum vector to the interaction point $<20\mu$m, and (iv) $x_{E_{D^{*+}}}$ >0.2 for the three-prong and satellite modes and $x_{E_{D^{*+}}}$ >0.4 for the five-prong mode.

For all D^{*+} "candidates we required the proper decay time of the D^0, $\tau_{\text{proper}} = L/\beta\sqrt{1-\beta^2}$, where $\beta = p_{D^0}/E_{D^0}$ and p_{D^0} and E_{D^0} are the momentum and energy respectively of the candidate D^0 meson, to be in the range $0< \tau_{\text{proper}} <$ 1ps. Figs. 2(a), (b) and (c) show the distribution of ΔM, where $\Delta M \equiv M^{cand}_{D^{*+}} - M^{cand}_{D^0}$, after the above cuts for the three D^0 decay modes, upon which is superimposed the Monte Carlo simulated distribution in which the flavor composition is shown[2]. The hemisphere was tagged as *c* if it contained a D^{*+} candidate with ΔM <0.15 GeV/c^2.

$D^+ \to K^-\pi^+\pi^+$ candidates were formed by combining two tracks of the same sign with one track of the opposite sign, where all three tracks were required to have momentum p >1 GeV/c. The two like-sign tracks were assigned π^+ masses, the opposite-sign track was given the K^- mass, and all three tracks were fitted to a common vertex. A series of cuts was applied to reject random combinatorics, D^{*+}, and B-decay backgrounds. We required: (i) x_{D^+} >0.4, (ii) $\cos\theta_{KD^+} > -0.8$, where θ_{KD^+} is the angle between the directions of the D^+ in the laboratory frame and the K^- in the D^+ rest frame, (iii) the mass differences $M(K^-\pi^+\pi^+) - M(K^-\pi^+)$ for each of the two pions to be greater than 0.16 GeV/c^2, (iv) the normalized D^+ decay length L^+/σ_{L^+} >3.0, and (v) the

[2]In the Monte Carlo simulation the production cross section and branching fractions, and normalization of the ΔM distributions in the region ΔM > 0.15 GeV/c^2, for the $D^0 \to K\pi$ and $D^0 \to K\pi\pi^0$ modes were adjusted to match the data in Fig. 2, as described in Ref. [19]. The adjustment was small and included in the systematic errors.

projected angle between the D^+ momentum vector and the vertex flight direction to be less than 5 mrad in the plane perpendicular to the beam axis and less than 20 mrad in the plane containing the beam axis. The hemisphere was *c*- tagged if it contained a $D^+ \to K^-\pi^+\pi^+$ candidate in the mass range 1.800 $\mathrm{GeV/c^2} < M(K^-\pi^+\pi^+) <$1.940 $\mathrm{GeV/c^2}$. Fig. 2(d) shows the mass $M(K^-\pi^+\pi^+)$ distribution of the data upon which is superimposed the Monte Carlo simulated distribution in which the flavor composition is shown.

The union of the three samples of D^{*+} candidates and the sample of D^+ candidates was used to tag *c* quark hemispheres. The flavor composition of these tagged hemispheres is shown in Table 1.

4 Measurement of Charged Multiplicities

Well-measured charged tracks defined in Section 2 were counted in the hemispheres opposite to those tagged. The measured average hemisphere multiplicities $\overline{m}_i (i =$ *uds, c, b)* were $\overline{m}_{uds}$ = 8.94 ± 0.01, $\overline{m}_c$ = 9.15 ± 0.12 and $\overline{m}_b$ = 9.99 ± 0.04 (statistical errors only).

The $\overline{m}_i$ are related to the true average multiplicities $\overline{n}_j (j =$ *uds, c, b)* of *uds, c* and *b* quark events by:

$$2 \times \overline{m}_i = P_{i,uds} C_{i,uds} \overline{n}_{uds} + P_{i,c}(C^{dk}_{i,c}\overline{n}^{dk}_c + C^{nl}_{i,c}\overline{n}^{nl}_c) + P_{i,b}(C^{dk}_{i,b}\overline{n}^{dk}_b + C^{nl}_{i,b}\overline{n}^{nl}_b) \qquad (1)$$

where: P_{ij} is the fraction of hemispheres of quark type *j* in the *i*- tagged hemisphere sample; $\overline{n}_j = \overline{n}^{dk}_j + \overline{n}^{nl}_j (j \neq$ *uds),* and $\overline{n}^{dk}_j$ is the true average multiplicity originating from the decay products of *j*- hadrons and $\overline{n}^{nl}_j$ is that originating from the non-leading particles; $C_{i,uds}$ is the ratio of the average number of measured charged tracks in light quark hemispheres opposite i-tagged hemispheres, to the average number of charged tracks in true light quark hemispheres; $C^{dk}_{i,j} (j \neq$ *uds)* is the ratio of the average number of measured charged tracks originating from the decay products of *j*- hadrons [3] in

[3] We include the products of both strongly and weakly decaying heavy hadrons.

j	uds	c		b	
i		dk	nl	dk	nl
uds	$0.875 \pm 0.001 \pm 0.001$	$0.798 \pm 0.002^{+0.006}_{-0.005}$	$0.885 \pm 0.002^{+0.013}_{-0.015}$	$0.820 \pm 0.002^{+0.024}_{-0.020}$	$0.887 \pm 0.003^{+0.022}_{-0.021}$
c	$0.803 \pm 0.019^{+0.005}_{-0.007}$	$0.831 \pm 0.011 \pm 0.004$	$0.864 \pm 0.009^{+0.014}_{-0.017}$	$0.854 \pm 0.013^{+0.030}_{-0.024}$	$0.849 \pm 0.015 \pm 0.026$
b	$0.875 \pm 0.015^{+0.005}_{-0.002}$	$0.816 \pm 0.013 \pm 0.003$	$0.887 \pm 0.010^{+0.016}_{-0.018}$	$0.854 \pm 0.003^{+0.025}_{-0.021}$	$0.893 \pm 0.004 \pm 0.025$

Table 2. The constants C calculated from the Monte Carlo simulation. The first quoted errors are statistical and arise from the finite size of the Monte Carlo sample. The second are due to the uncertainties from C and B hadron production and decay.

hemispheres opposite to *i*- tagged hemispheres, to the average number of tracks originating from the decay products of *j*- hadrons; $C^{nl}_{i,j}$ $(j \neq uds)$ is the ratio of the average number of measured charged tracks originating from the non-leading particles in true *j*- quark hemispheres opposite to those tagged as *i*- quark hemispheres, to the average number of tracks originating from non-leading particles in true *j*- quark hemispheres. The constants P are shown in Table 1. The constants C were also calculated from our Monte Carlo simulation and are shown in Table 2: they account for the effects of detector acceptance and inefficiencies, for tracks from beam-related backgrounds and interactions in the detector material, and for biases introduced by the event and tagged-sample selection criteria. We included in the generated multiplicity any prompt charged track with mean lifetime greater than 3×10^{-10}s. or any charged decay product with mean lifetime greater than 3×10^{-10}s of a particle with mean lifetime less than 3×10^{-10}s.

We fixed $\overline{n}_c^{dk} = 5.20$ and $\overline{n}_b^{dk} = 11.10$, using the measured values from [20, 21, 22] with the addition of 0.20 and 0.22 tracks, respectively, estimated from the Monte Carlo simulation, to account for the effects of higher mass states of heavy hadrons produced in Z^0 decays.

We then solved eqns. (1) to obtain the average charged multiplicities per event, $\overline{n}_{uds} = 20.21 \pm 0.10$, $\overline{n}_c = 21.28 \pm 0.46$ and $\overline{n}_b = 23.14 \pm 0.10$ (statistical errors only). The multiplicity differences between c and light quark events, and b and light quark

Source of Uncertainty	$\overline{n}_{uds}$	$\overline{n}_c$	$\overline{n}_b$	$\Delta\overline{n}_c$	$\Delta\overline{n}_b$
Tracking efficiency	±0.121	±0.129	±0.137	±0.008	±0.016
γ conversion & fake tracks	±0.101	±0.108	±0.114	±0.007	±0.013
Monte Carlo statistics	±0.046	±0.212	±0.045	±0.217	±0.064
Total	±0.164	±0.271	±0.184	±0.217	±0.067

Table 3. Systematic errors due to detector modelling.

events are, respectively

$$\Delta\overline{n}_c = 1.07 \pm 0.47\ (\text{stat.})$$
$$\Delta\overline{n}_b = 2.93 \pm 0.14\ (\text{stat.})$$

5 Systematic Errors

Experimental systematic errors arise from uncertainties in modelling the acceptance, efficiency and resolution of the detector. Systematic uncertainties also arise from errors on the experimental measurements that function as the input parameters to the modelling of the underlying physics processes, such as errors on the modelling of *b* and *c* fragmentation and decays of B and C hadrons.

The effect of uncertainty in the tracking efficiency was estimated to cause a common ±0.6% variation of the constants *C*. The effect of uncertainty in the corrections for the residual γ conversions and fake tracks was estimated to cause a common ±0.5% variation of the constants *C*. Statistical effects from the limited Monte Carlo sample size were also considered. These errors, summarized in Table 3, were added in quadrature to obtain a total systematic error due to detector modelling. Note that the uncertainties in total track reconstruction efficiency are a dominant source of systematic error for $\overline{n}_{uds}$ and $\overline{n}_b$, but are small for the differences $\Delta\overline{n}_c$ and $\Delta\overline{n}_b$. In the case of $\overline{n}_c, \Delta\overline{n}_c$ and $\Delta\overline{n}_b$ the statistical error from the limited Monte Carlo sample size is dominant.

We performed several consistency checks on our results. We checked that our Monte Carlo simulation showed good agreement with the data for track $p_\perp$ and $\cos\theta$

distributions in the hemispheres opposite to those tagged. We then varied the thrust axis containment cut within $0.5 \leq |\cos\theta_T| \leq 0.8$. To check for possible bias from our hemisphere tags the cut on the track significance δ_{norm} was varied from 2.0 to 4.0 for the light and *b* quark hemisphere tags, and D^{*+} and D^+ mesons were considered separately as a *c* quark hemisphere tag. Finally, we performed our analysis separately in 2- and $\geq$ 3-jet event samples selected using the Durham algorithm [23] with $y_{cut}=0.003$, to check for any possible bias in multi-jet events. In each case all the re-evaluated $\overline{n}_i$ were found to be consistent with our central values of $\overline{n}_i$ within the statistical errors.

In order to estimate the systematic errors due to uncertainties in modelling heavy hadron production and decay we used an event re-weighting scheme to vary the multiplicity distributions in the Monte Carlo simulation and to obtain modified values of the constants *C* and *P*. The effect of uncertainty in heavy flavor fragmentation was estimated by varying the ϵ parameter of the Peterson fragmentation function [24] used as input to generate the Monte Carlo sample, corresponding to $\delta < x_E > = \pm 0.012$ and ± 0.011 for *c* and *b* quarks respectively, corresponding to the average errors in measurements of these quantities [25]. The average B hadron lifetime was varied by ±0.1 ps for B mesons and ± 0.3 ps for B baryons [26]. The effect of varying the B baryon production rate in *b* events by $\pm 3\%$ [16] was also examined. Absolute variations of $\pm 6\%$ and $\pm 4\%$ were applied to the $B \to D^+$ branching ratio and $c \to D^+$ branching ratio, respectively [16]. The effect of the present experimental uncertainties in the branching fractions, $R_c = \Gamma(Z^0 \to c\bar{c})/\Gamma(Z^0 \to q\bar{q})$ and $R_b = \Gamma(Z^0 \to b\bar{b})/\Gamma(Z^0 \to q\bar{q})$, of $\delta R_c = \pm 0.020$ and $\delta R_b = \pm 0.003$ respectively [26] were also included. The decay multiplicities of C and B hadrons were varied by ± 0.26 and ± 0.36 charged tracks, respectively [20, 21, 22]. For the D^{*+} analysis we also accounted for the adjustment of the production cross section and branching fractions for the $D^0 \to K\pi$ and $D^0 \to K\pi\pi^0$ modes in the Monte Carlo by assigning the full shift of the Monte Carlo simulated distribution as a systematic error. These uncertainties, summarized in Table 4, were added in quadrature to obtain total systematic uncertainties due to C and B hadron modelling. For $\Delta\overline{n}_c (\Delta\overline{n}_b)$ the

Source of Uncertainty	Variation	$\overline{n}_{uds}$	$\overline{n}_c$	$\overline{n}_b$	$\Delta\overline{n}_c$	$\Delta\overline{n}_b$
b fragmentation	$\langle x_{E_b}\rangle$=0.700±0.011	±0.001	$^{+0.002}_{-0}$	$^{+0.288}_{-0.281}$	$^{+0.004}_{-0}$	$^{+0.289}_{-0.279}$
B meson lifetime	τ_b=1.55±0.1 ps	±0.001	$^{+0.027}_{-0.028}$	$^{+0.010}_{-0.007}$	$^{+0.027}_{-0.026}$	$^{+0.012}_{-0.007}$
B baryon lifetime	τ_b=1.10±0.3 ps	$^{+0}_{-0.008}$	$^{+0.032}_{-0.036}$	$^{+0.008}_{-0.001}$	$^{+0.041}_{-0}$	$^{+0.012}_{-0}$
B baryon prod. rate	f_{Λ_b} = 9% ± 3%	$^{+0.004}_{-0.001}$	$^{+0}_{-0.001}$	$^{+0.021}_{-0.020}$	$^{+0.001}_{-0.003}$	$^{+0.019}_{-0.018}$
R_b (b fraction)	0.221±0.003	±0.001	$^{+0.007}_{-0.006}$	$^{+0.041}_{-0.040}$	$^{+0.007}_{-0.008}$	$^{+0.040}_{-0.039}$
$B \to D^+ + X$ fraction	0.17±0.06	$^{+0}_{-0.007}$	$^{+0.054}_{-0}$	$^{+0}_{-0.036}$	$^{+0.053}_{-0}$	$^{+0}_{-0.024}$
c fragmentation	$\langle x_{E_c}\rangle$=0.494±0.012	$^{+0.008}_{-0.010}$	$^{+0.236}_{-0.155}$	$^{+0.004}_{-0.002}$	$^{+0.244}_{-0.151}$	$^{+0.015}_{-0.008}$
R_c (c fraction)	0.171±0.020	$^{+0.026}_{-0.027}$	$^{+0.081}_{-0.099}$	$^{+0.006}_{-0.007}$	$^{+0.107}_{-0.126}$	±0.033
$c\bar{c} \to D^+ + X$ fraction	0.20±0.04	$^{+0.004}_{-0.003}$	$^{+0.035}_{-0.039}$	±0.006	$^{+0.039}_{-0.042}$	$^{+0.010}_{-0.009}$
$\overline{n}_c^{dk}$	5.20±0.26	±0.003	$^{+0.010}_{-0.009}$	$^{+0.001}_{-0}$	$^{+0.005}_{-0.006}$	±0.003
$\overline{n}_b^{dk}$	11.10±0.36	±0.003	$^{+0.009}_{-0.008}$	±0.016	±0.012	±0.013
$D^0 \to K\pi$, $D^0 \to K\pi\pi^0$ production	−20%	−0.013	+0.062	−0.003	+0.075	+0.010
Total		$^{+0.028}_{-0.034}$	$^{+0.269}_{-0.194}$	$^{+0.293}_{-0.287}$	$^{+0.289}_{-0.203}$	$^{+0.296}_{-0.286}$

Table 4. Systematic uncertainties due to heavy hadron modelling.

dominant contributions were from the uncertainties in *c (b)* fragmentation and $R_c(R_b)$.

6 Summary and Conclusions

Combining systematic uncertainties in quadrature we obtain:

$$\begin{aligned}
\overline{n}_{uds} &= 20.21 \pm 0.10\ (\text{stat.}) \pm 0.17\ (\text{syst.}) \\
\overline{n}_c &= 21.28 \pm 0.46\ (\text{stat.})^{+0.38}_{-0.33}\ (\text{syst.}) \\
\overline{n}_b &= 23.14 \pm 0.10\ (\text{stat.})^{+0.35}_{-0.34}\ (\text{syst.}).
\end{aligned}$$

The hypothesis of flavor-independent fragmentation implies that $\overline{n}_Q^{nl}([1-\langle x_{E_Q}(W)\rangle]W) \equiv \overline{n}_Q(W) - \overline{n}_Q^{dk} = \overline{n}_{uds}([1 - \langle x_{E_Q}(W)\rangle]W)$. Subtracting $\overline{n}_c^{dk}$=5.20 and $\overline{n}_b^{dk}$=11.10 from our measured $\overline{n}_c$ and $\overline{n}_b$, we obtained $\overline{n}_c^{nl}$ = 16.08 ± 0.46(stat.) $^{+0.38}_{-0.33}$(syst.) and $\overline{n}_b^{nl}$ = 12.04 ± 0.10(stat.) $^{+0.35}_{-0.34}$ (syst.), respectively. Fig. 3(a) shows our measurements of $\overline{n}_{uds}$ at

$W = M_Z$ and of $\overline{n}_c^{nl}$ and $\overline{n}_b^{nl}$ plotted at the appropriately reduced non-leading energy $[1 - \langle x_{E_Q}(W)\rangle]W$. Previous measurements of these quantities [1, 6, 7, 8, 9, 10, 27, 28] are also shown. The solid curve is a fit to the $\overline{n}_{uds}$ measurements shown combined with those at 5< W < 92 GeV [27]: Fig. 3(b) shows the differences between the non-leading data points in Fig. 3(a) and the solid curve. A linear fit to these differences (Fig. 3(b)) yields a slope of s = 1.54 ± 0.41 tracks/ln(GeV), inconsistent with the hypothesis of identical energy dependence (s = 0.0) at the level of 3.8 standard deviations, indicating that the hypothesis of flavor-independent fragmentation is disfavored at this level.

Combining systematic uncertainties in quadrature we obtain:

$$\Delta\overline{n}_c = 1.07 \pm 0.47\ (\text{stat.})^{+0.36}_{-0.30}\ (\text{syst.})$$
$$\Delta\overline{n}_b = 2.93 \pm 0.14\ (\text{stat.})^{+0.30}_{-0.29}\ (\text{syst.})$$

Fig. 4 shows our measurements of $\Delta\overline{n}_c$ and $\Delta\overline{n}_b$ together with those from other experiments [1, 6, 7, 8, 9, 10, 27], at the respective center-of-mass energies. The new result for $\Delta\overline{n}_b$ is consistent with our previous measurement [5] and with the measurements from LEP [9, 10] and Mark-II [27], and that for $\Delta\overline{n}_c$ is consistent with the OPAL measurement [10].

Within errors all data points in Fig. 4(a) or 4(b) are consistent with the notion of energy independence of $\Delta\overline{n}_Q$, but disfavor the flavor-independent fragmentation hypothesis, which implies that $\Delta\overline{n}_Q$ decreases with W in proportion to $\overline{n}_{uds}(W)$. Because of different measurement techniques, results for $\Delta\overline{n}_c$ and $\Delta\overline{n}_b$ at PEP, PETRA and LEP are largely uncorrelated with our results. Linear fits to the $\Delta\overline{n}_c$ and $\Delta\overline{n}_b$ data as a function of ln (W) yield slopes of $s = -1.33 \pm 1.04$ and $s = -1.43 \pm 0.82$ tracks/ln(GeV), respectively. These slopes are consistent with the perturbative QCD prediction of Ref. [3], s =0, at the level of 1.3 and 1.7 standard deviations, respectively

Comparing our measurements of $\Delta\overline{n}_c$ and $\Delta\overline{n}_b$ with the predictions for their absolute values (Fig. 4) we found that both were in good agreement with the predictions of Ref. [4], while the former was in good agreement with the expectation of Ref. [3], and the latter within 1.7σ of this prediction.

As a result of the accurate measurements of $\Delta\overline{n}_c$ and $\Delta\overline{n}_b$ at $W = M_Z$, constraints on the energy independence of these quantities are now limited by the uncertainty in the lower energy measurements. In order to improve the constraints on the validity of perturbative QCD down to the scales M_b^2 or M_c^2, it is necessary to improve the accuracy of the measurements of $\Delta\overline{n}_b$ and $\Delta\overline{n}_c$, respectively, at lower energies, and/or extend the ln *(W)* lever-arm of such measurements. It would thus be desirable to have measurements of $\Delta\overline{n}_c$ from the continuum below the $\Upsilon(4S)$ performed at the existing and planned B factories, and for both $\Delta\overline{n}_c$ and $\Delta\overline{n}_b$ to be measured at LEP-II and e^+e^- colliders at even higher energies.

Acknowledgements

We thank the personnel of the SLAC accelerator department and the technical staffs of our collaborating institutions for their outstanding efforts on our behalf.

References

[1] Mark-II Collaboration, P.C. Rowson *et al.,* Phys. Rev. Lett. **54** (1985) 2580.

[2] A.V. Kisselev *et al.,* Z. Phys. **C41** (1988) 521.

[3] B.A. Schumm *et al.,* Phys. Rev. Lett. **69** (1992) 3025.

[4] V.A. Petrov and A.V. Kisselev, Z. Phys. **C66** (1995) 453.

[5] SLD Collaboration, K. Abe *et al.,* Phys. Rev. Lett. **72** (1994) 3145.

[6] DELCO Collaboration, M. Sakuda *et al.,* Phys. Lett. **B152** (1985) 399.

[7] TPC Collaboration, H. Aihara *et al.,* Phys. Lett. **B134** (1987) 299.

[8] TASSO Collaboration, W. Braunschweig *et al.,* Z. Phys. **C42** (1989) 17.
M. Althoff *et al.,* Phys. Lett. **B135** (1984) 243.

[9] DELPHI Collaboration, P. Abreu *et al.,* Phys. Lett. **B347** (1995) 447.

[10] OPAL Collaboration, R. Akers *et al.,* Phys. Lett. **B352** (1995) 176.

[11] SLD Design Report, SLAC Report **273** (1984).

[12] SLD Collaboration, K. Abe *et al.,* Phys. Rev. **D51** (1995) 962.

[13] M.D. Hildreth *et al.,* Nucl. Inst. Meth. **A367** (1995) 111.

[14] C. J. S. Damerell *et al.,* Nucl. Inst. Meth. **A288** (1990) 288.

[15] S. Brandt *et al.,* Phys. Lett. **12** (1964) 57.
E. Farhi, Phys. Rev. Lett. **39** (1977) 1587.

[16] SLD Collaboration, K. Abe *et al.,* Phys. Rev. **D53** (1996) 1023.

[17] T. Sjöstrand, CERN-TH.7112/93 (1993).

[18] P.N. Burrows, Z. Phys. **C41** (1988) 375; OPAL Collaboration, M.Z. Akrawy *et al., ibid.,* **C47** (1990) 505.

[19] SLD Collaboration, K. Abe *et al.,* Phys. Rev. Lett. **75** (1995) 3609.

[20] Mark-III Collaboration, D. Coffman *et al.,* Phys. Lett. **B263** (1991) 13.5.

[21] B. Gittelman and S. Stone, in *High Energy Electron-Positron Physics*, edited by A. Ali and P. Söding (World Scientific, Singapore, 1988), p. 273.

[22] ARGUS Collaboration, H. Albrecht *et al.*, Z. Phys. **C54** (1992) 13.

[23] S. Bethke *et al.*, Nucl. Phys. **B370** (1992) 310.

[24] C. Peterson *et al.*, Phys. Rev. **D27** (1983) 105.

[25] ALEPH Collaboration, D. Buskulic *et al.*, Z. Phys. **C62** (1994) 1;
ALEPH Collaboration, D. Buskulic *et al.*, Z. Phys. **C62** (1994) 179;
L3 Collaboration, B. Adeva *et al.*, Phys. Lett. **B261** (1991) 177;
OPAL Collaboration, R. Akers *et al.*, Z. Phys. **C60** (1993) 199;
OPAL Collaboration, R. Akers *et al.*, Z. Phys. **C60** (1993) 601;
OPAL Collaboration, R. Akers *et al.*, Z. Phys. **C61** (1994) 209;
DELPHI Collaboration, P. Abreu *et al.*, Z. Phys. **C59** (1993) 533.

[26] Particle Data Group, L. Montanet *et al.*, Phys. Rev. **D50** Part I (1994).

[27] Mark-II Collaboration, B.A. Schumm *et al.*, Phys. Rev. **D46** (1992) 453.

[28] TOPAZ Collaboration, K. Nagai *et al.*, Phys. Lett. **B278** (1992) 506.

** K. Abe,[19] K. Abe,[29] I. Abt,[13] T. Akagi,[27] N.J. Allen,[4] W.W. Ash,[27]†
D. Aston,[27] K.G. Baird,[24] C. Baltay,[33] H.R. Band,[32] M.B. Barakat,[33]
G. Baranko,[9] O. Bardon,[15] T. Barklow,[27] A.O. Bazarko,[10] R. Ben-David,[33]
A.C. Benvenuti,[2] G.M. Bilei,[22] D. Bisello,[21] G. Blaylock,[6] J.R. Bogart,[27]
B. Bolen,[17] T. Bolton,[10] G.R. Bower,[27] J.E. Brau,[20] M. Breidenbach,[27]
W.M. Bugg,[28] D. Burke,[27] T.H. Burnett,[31] P.N. Burrows,[15] W. Busza,[15]
A. Calcaterra,[12] D.O. Caldwell,[5] D. Calloway,[27] B. Camanzi,[11] M. Carpinelli,[23]
R. Cassell,[27] R. Castaldi,[23][a] A. Castro,[21] M. Cavalli-Sforza,[6] A. Chou,[27]
E. Church,[31] H.O. Cohn,[28] J.A. Coller,[3] V. Cook,[31] R. Cotton,[4]
R.F. Cowan,[15] D.G. Coyne,[6] G. Crawford,[27] A. D'Oliveira,[7] C.J.S. Damerell,[25]
M. Daoudi,[27] R. De Sangro,[12] R. Dell'Orso,[23] P.J. Dervan,[4] M. Dima,[8]
D.N. Dong,[15] P.Y.C. Du,[28] R. Dubois,[27] B.I. Eisenstein,[13] R. Elia,[27]
E. Etzion,[4] D. Falciai,[22] C. Fan,[9] M.J. Fero,[15] R. Frey,[20] K. Furuno,[20]
T. Gillman,[25] G. Gladding,[13] S. Gonzalez,[15] G.D. Hallewell,[27] E.L. Hart,[28]
J.L. Harton,[8] A. Hasan,[4] Y. Hasegawa,[29] K. Hasuko,[29] S. J. Hedges,[3]
S.S. Hertzbach,[16] M.D. Hildreth,[27] J. Huber,[20] M.E. Huffer,[27] E.W. Hughes,[27]
H. Hwang,[20] Y. Iwasaki,[29] D.J. Jackson,[25] P. Jacques,[24] J. A. Jaros,[27]
A.S. Johnson,[3] J.R. Johnson,[32] R.A. Johnson,[7] T. Junk,[27] R. Kajikawa,[19]
M. Kalelkar,[24] H. J. Kang,[26] I. Karliner,[13] H. Kawahara,[27] H.W. Kendall,[15]
Y. D. Kim,[26] M.E. King,[27] R. King,[27] R.R. Kofler,[16] N.M. Krishna,[9]
R.S. Kroeger,[17] J.F. Labs,[27] M. Langston,[20] A. Lath,[15] J.A. Lauber,[9]
D.W.G.S. Leith,[27] V. Lia,[15] M.X. Liu,[33] X. Liu,[6] M. Loreti,[21] A. Lu,[5]
H.L. Lynch,[27] J. Ma,[31] G. Mancinelli,[22] S. Manly,[33] G. Mantovani,[22]
T.W. Markiewicz,[27] T. Maruyama,[27] H. Masuda,[27] E. Mazzucato,[11]
A.K. McKemey,[4] B.T. Meadows,[7] R. Messner,[27] P.M. Mockett,[31]
K.C. Moffeit,[27] T.B. Moore,[33] D. Muller,[27] T. Nagamine,[27] S. Narita,[29]
U. Nauenberg,[9] H. Neal,[27] M. Nussbaum,[7] Y. Ohnishi,[19] L.S. Osborne,[15]
R.S. Panvini,[30] H. Park,[20] T.J. Pavel,[27] I. Peruzzi,[12][b] M. Piccolo,[12]

L. Piemontese,[11] E. Pieroni,[23] K.T. Pitts,[20] R.J. Plano,[24] R. Prepost,[32]
C.Y. Prescott,[27] G.D. Punkar,[27] J. Quigley,[15] B.N. Ratcliff,[27] T.W. Reeves,[30]
J. Reidy,[17] P.E. Rensing,[27] L.S. Rochester,[27] P.C. Rowson,[10] J.J. Russell,[27]
O.H. Saxton,[27] T. Schalk,[6] R.H. Schindler,[27] B.A. Schumm,[14] S. Sen,[33]
V.V. Serbo,[32] M.H. Shaevitz,[10] J.T. Shank,[3] G. Shapiro,[14] D.J. Sherden,[27]
K.D. Shmakov,[28] C. Simopoulos,[27] N.B. Sinev,[20] S.R. Smith,[27] M.B. Smy,[8]
J.A. Snyder,[33] P. Stamer,[24] H. Steiner,[14] R. Steiner,[1] M.G. Strauss,[16] D. Su,[27]
F. Suekane,[29] A. Sugiyama,[19] S. Suzuki,[19] M. Swartz,[27] A. Szumilo,[31]
T. Takahashi,[27] F.E. Taylor,[15] E. Torrence,[15] A.I. Trandafir,[16] J.D. Turk,[33]
T. Usher,[27] J. Va'vra,[27] C. Vannini,[23] E. Vella,[27] J.P. Venuti,[30] R. Verdier,[15]
P.G. Verdini,[23] S.R. Wagner,[27] A.P. Waite,[27] S.J. Watts,[4] A.W. Weidemann,[28]
E.R. Weiss,[31] J.S. Whitaker,[3] S.L. White,[28] F.J. Wickens,[25] D.A. Williams,[6]
D.C. Williams,[15] S.H. Williams,[27] S. Willocq,[33] R.J. Wilson,[8]
W.J. Wisniewski,[27] M. Woods,[27] G.B. Word,[24] J. Wyss,[21] R.K. Yamamoto,[15]
J.M. Yamartino,[15] X. Yang,[20] S.J. Yellin,[5] C.C. Young,[27] H. Yuta,[29]
G. Zapalac,[32] R.W. Zdarko,[27] C. Zeitlin,[20] and J. Zhou,[20]

[1] *Adelphi University, Garden City, New York 11530*

[2] *INFN Sezione di Bologna, I-40126 Bologna, Italy*

[3] *Boston University, Boston, Massachusetts 02215*

[4] *Brunel University, Uxbridge, Middlesex UB8 3PH, United Kingdom*

[5] *University of California at Santa Barbara, Santa Barbara, California 93106*

[6] *University of California at Santa Cruz, Santa Cruz, California 95064*

[7] *University of Cincinnati, Cincinnati, Ohio 45221*

[8] *Colorado State University, Fort Collins, Colorado 80523*

[9] *University of Colorado, Boulder, Colorado 80309*

[10] *Columbia University, New York, New York 10027*

[11] *INFN Sezione di Ferrara and Università di Ferrara, I-44100 Ferrara, Italy*

[12] *INFN Lab. Nazionali di Frascati, I-00044 Frascati, Italy*

[13] *University of Illinois, Urbana, Illinois 61801*

[14] *Lawrence Berkeley Laboratory, University of California, Berkeley, California 94720*

[15] *Massachusetts Institute of Technology, Cambridge, Massachusetts 02139*

[16] *University of Massachusetts, Amherst, Massachusetts 01003*

[17] *University of Mississippi, University, Mississippi 38677*

[19] *Nagoya University, Chikusa-ku, Nagoya 464 Japan*

[20] *University of Oregon, Eugene, Oregon 97403*

[21] *INFN Sezione di Padova and Università di Padova, I-35100 Padova, Italy*

[22] *INFN Sezione di Perugia and Università di Perugia, I-06100 Perugia, Italy*

[23] *INFN Sezione di Pisa and Università di Pisa, I-56100 Pisa, Italy*

[24] *Rutgers University, Piscataway, New Jersey 08855*

[25] *Rutherford Appleton Laboratory, Chilton, Didcot, Oxon OX11 0QX United Kingdom*

[26] *Sogang University, Seoul, Korea*

[27] *Stanford Linear Accelerator Center, Stanford University, Stanford, California 94309*

[28] *University of Tennessee, Knoxville, Tennessee 37996*

[29] *Tohoku University, Sendai 980 Japan*

[30] *Vanderbilt University, Nashville, Tennessee 37235*

[31] *University of Washington, Seattle, Washington 98195*

[32] *University of Wisconsin, Madison, Wisconsin 53706*

[33] *Yale University, New Haven, Connecticut 06511*

† *Deceased*

[a] *Also at the Università di Genova*

[b] *Also at the Università di Perugia*

Figure captions

Figure 1. The distribution of the number of tracks per hemisphere n_{sig} which miss the interaction point by more than 3σ in the *x-y* plane. The points represent the data distribution and the solid histogram represents the Monte Carlo sample. The flavor composition of the Monte Carlo distribution is shown.

Figure 2. The distributions of ΔM for a) $D^0 \to K\pi$, b) $D^0 \to K\pi\pi^0$ and c) $D^0 \to K\pi\pi\pi$; d) $M(K\pi\pi)$ distribution for $D^+ \to K\pi\pi$ (see text). The points represent the data distributions and the solid histograms represent the Monte Carlo simulated distributions. The flavor composition of the Monte Carlo distributions are shown.

Figure 3. a) Our measurements of $\overline{n}_{uds}$ at $W = M_Z$ and the non-leading multiplicities $\overline{n}_c^{nl}$ and $\overline{n}_b^{nl}$ plotted at the appropriately reduced non-leading energy $[1 - \langle x_{E_Q}(W)\rangle]W$. Previous measurements of these quantities [1, 6, 7, 8, 9, 10, 27, 28] are also shown. The solid curve is a fit [27] to $\overline{n}_{uds}$ measured in the range $5 < W < 92$ GeV. The error on this curve (dotted lines) is dominated by the uncertainty on the removal of the heavy quark contribution to each measured total charged multiplicity. b) The differences (points) between the non-leading data points in a) and the solid curve. A linear fit to the these differences is shown by the dashed line. For clarity the data points from the Z^0 experiments are displayed with small relative displacements in W.

Figure 4. Differences in average total multiplicities a) $\Delta\overline{n}_c$ and b) $\Delta\overline{n}_b$ as functions of center-of-mass energy. The predictions of Ref. [3] are shown as the solid lines and those of Ref. [4] are shown as the dashed lines. For clarity the data points from the Z^0 experiments are displayed with small relative displacements in *W*.

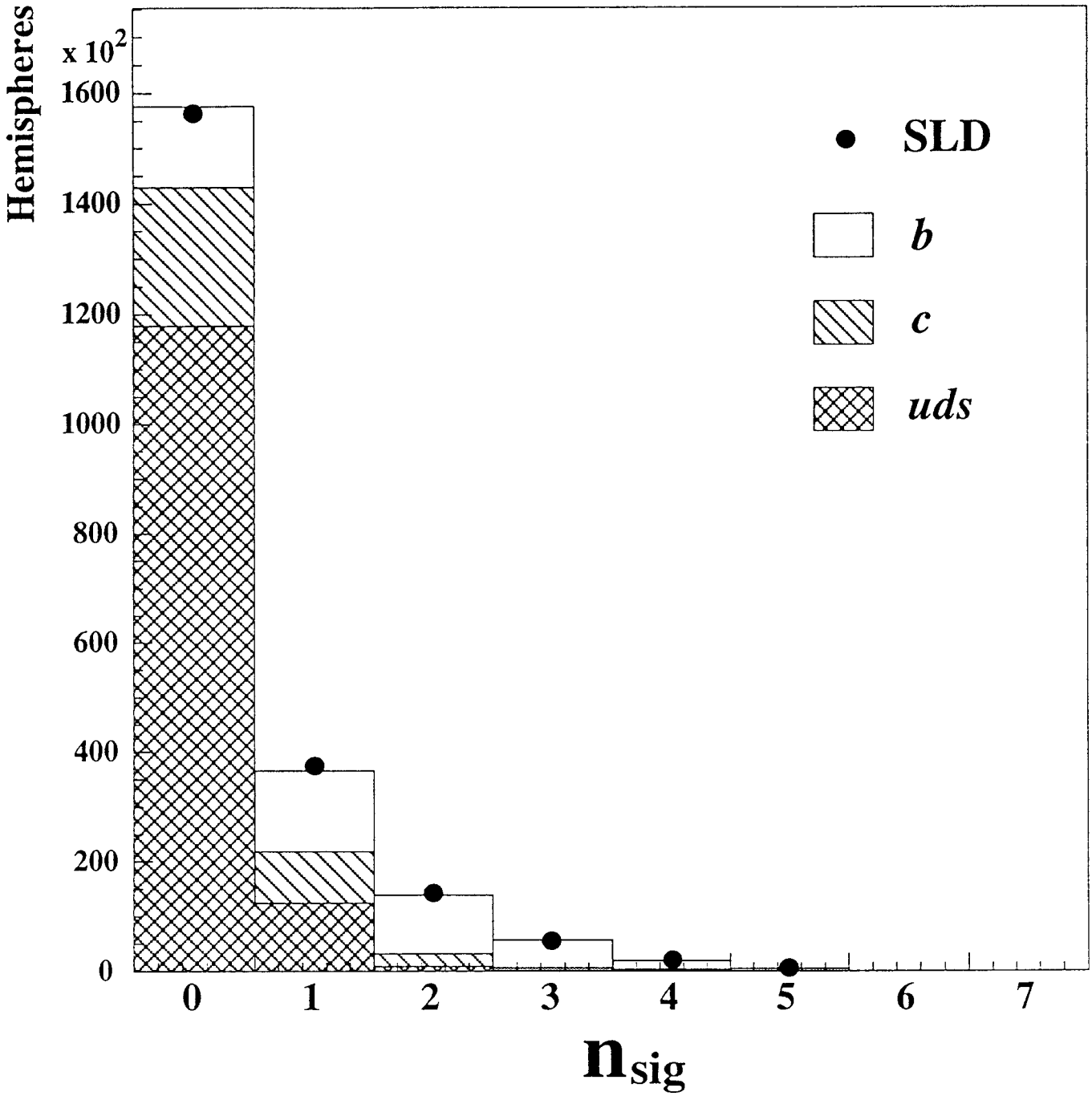
Hemispheres
x 10^2
1600
1400
1200
1000
800
600
400
200
0
SLD
b
c
uds
0
1
2
3
4
5
6
7
n_sig

Figure 1

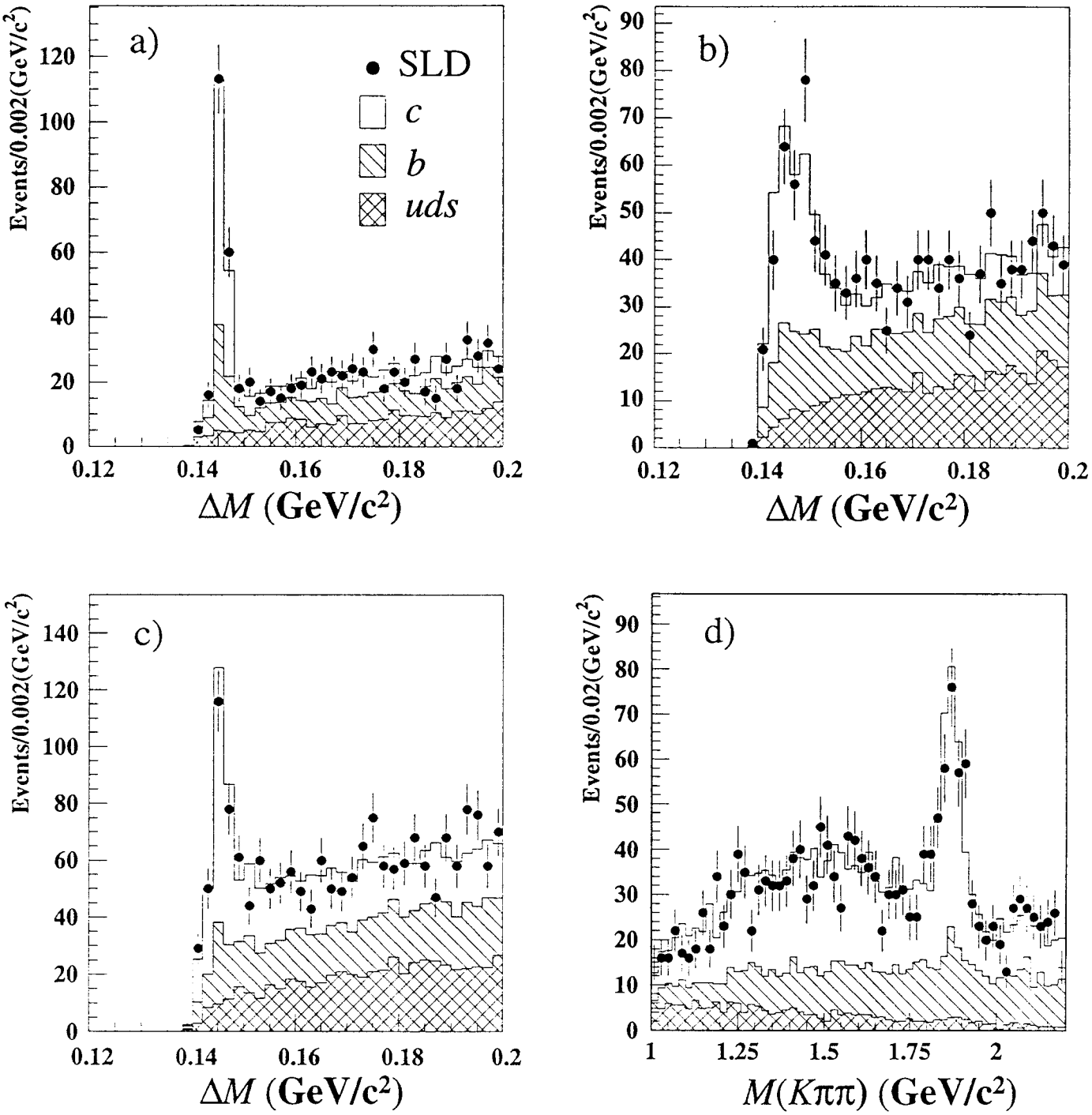
a)
SLD
c
b
uds
Events/0.002(GeV/c²)
ΔM (GeV/c²)
b)
Events/0.002(GeV/c²)
ΔM (GeV/c²)
c)
Events/0.002(GeV/c²)
ΔM (GeV/c²)
d)
Events/0.02(GeV/c²)
M(Kππ) (GeV/c²)

Figure 2

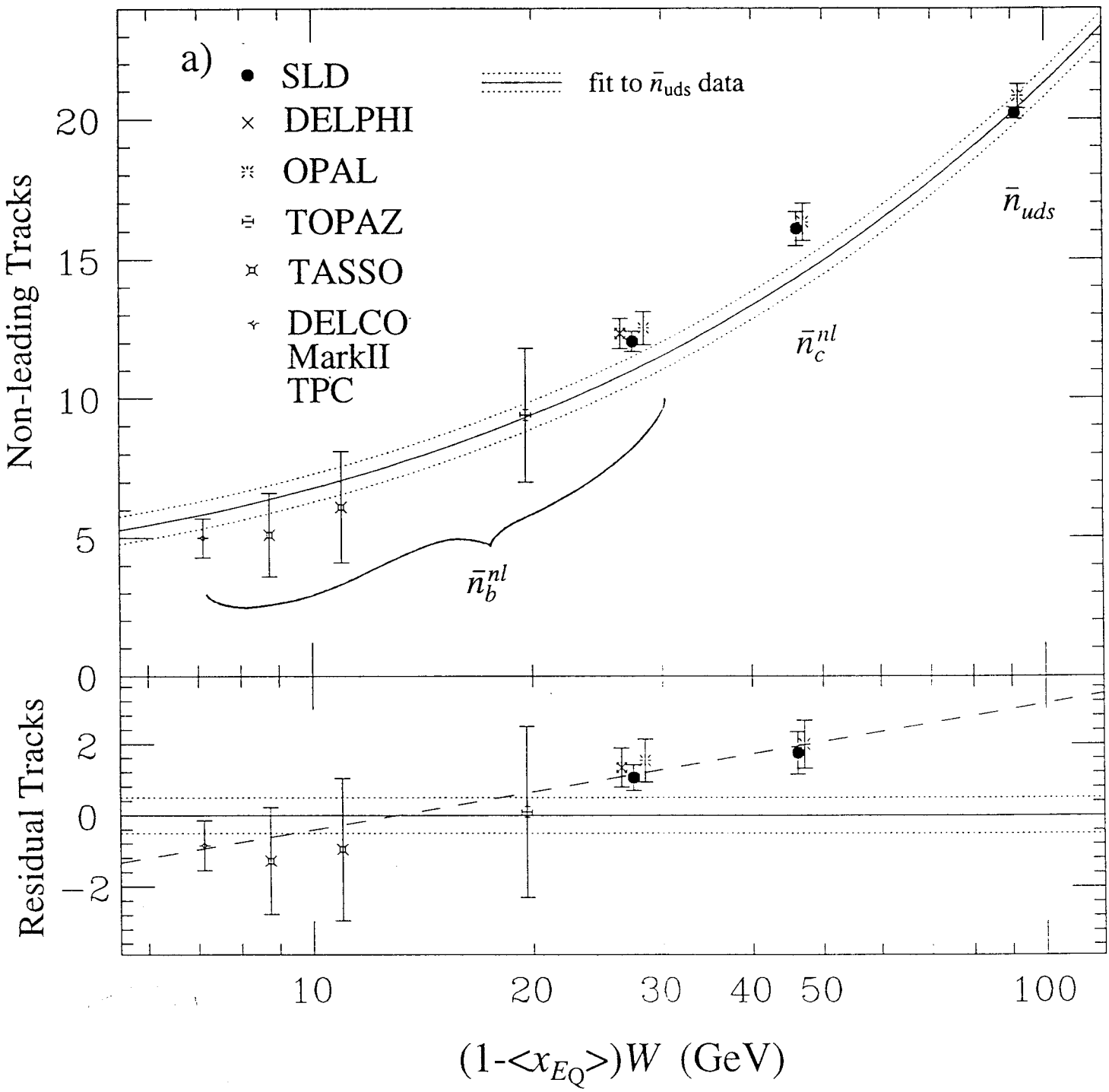
a)
SLD
DELPHI
OPAL
TOPAZ
TASSO
DELCO
MarkII
TPC
fit to $\bar{n}_{uds}$ data
$\bar{n}_{uds}$
$\bar{n}_c^{nl}$
$\bar{n}_b^{nl}$
Non-leading Tracks
Residual Tracks
$(1-\langle x_{EQ}\rangle)W$ (GeV)

Figure 3

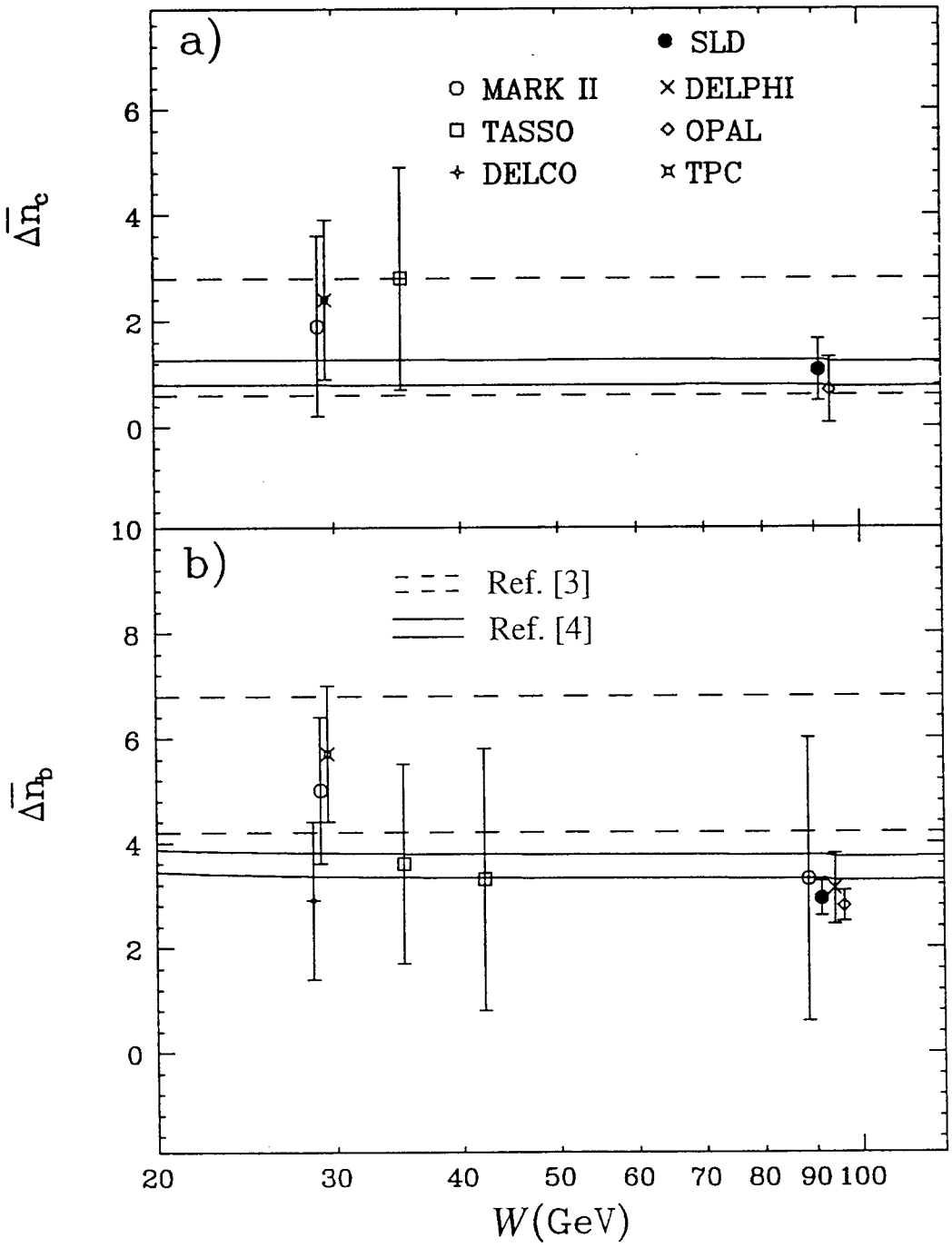
a)
SLD
MARK II
DELPHI
TASSO
OPAL
DELCO
TPC
$\overline{\Delta n}_c$
b)
Ref. [3]
Ref. [4]
$\overline{\Delta n}_b$
W(GeV)

Figure 4